Dynamic Stability of a Parachuting Payload.

Ezra Scher, RAFAEL- ISRAEL

ABSTRACT

The stability of motion of a parachuting payload, descending and rotating simultaneously, is affected by physical and design parameters. This paper presents an analysis of the behavior of this type of a system and its sensitivity to several parameters. The results from the ADAMS complete model have a good correlation with test results. A simplified analytic model does not represent the correct stability criteria, since it does not include the whole effects of the system.

INTRODUCTION

The stability of a parachuting payload, descending and rotating simultaneously, depends on several parameters - physical, geometrical and aerodynamicals. An example of the importance of a stable motion is in a Data Collection System (DCS) where the stability affects the area coverage efficiency. An analysis was performed, using ADAMS, to simulate this behavior. The analysis results were compared to experimental data. Furthermore, an analytic solution of a reduced system emphasized its insufficient accuracy and the need for a complete and accurate model.
The following topics will be considered in the paper:
- Description of the actual parts (payload, two arms and a parachute), physical and geometrical data (mass, center of mass and moments of inertia) and external loads. The aerodynamic coefficients were measured in a wind tunnel.
- The influence of moments of inertia, imbalance, tolerances and gaps on the stability of motion.
- The main results of the simulation, including comparison with experimental results.
- The results and limitations of the simple analytic model in comparison with the complete numerical model.
The major conclusions from the analysis are:
- Moment of inertia and gaps between the arms affect the stability range.
- Imbalance in the specified range has no effect on the stability.

MODEL DESCRIPTION

The system consists of four bodies as described in Figure 1:
- Generalized parachute
- Long Arm
- Short Arm
- Rotor (hanged payload).
The system has 9 to 12 Degrees of Freedom (DOF), depending upon the scenario to be tested. Nine DOF are inherent to the model, allocated as follows:
- Six DOF of the generalized parachute (three translationals and three rotationals DOF).
- One angular DOF of pitch angle between generalized parachute and long arm.
- One angular DOF of pitch angle between long arm and short arm.
- One angular DOF of pitch angle between short arm and rotor.

Three additional angular DOF, perpendicular to the three pitch DOF, represent gaps between the parts due to dimensional tolerances. The gaps, of about 0.5 [degs] each, enable these DOF to act in their limited range by applying impact forces between parts, when striking the stoppers. The physical and geometrical data were calculated and the aerodynamic coefficients were measured in wind tunnel experiments.

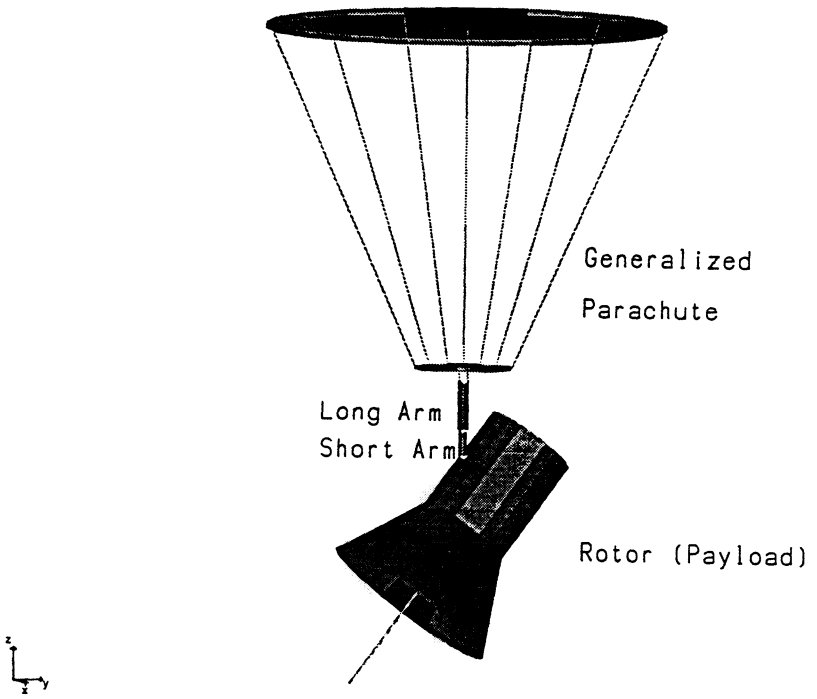

Figure 1 : General view of the model

COORDINATE SYSTEMS

Three major coordinate systems are to used in the model, as described in Figure 2.

- Global (inertial) coordinate system (X_G, Y_G, Z_G). The tip of the generalized parachute coincides with the global origin at time=0 of the analysis (point A, Figure 2).
- Local coordinate system (X_R, Y_R, Z_R) of the rotor defined at the point of connection between the short arm and the rotor (point B, Figure 2). X_R is parallel to the longitudinal axis of the rotor, Z_R axis is parallel to the pitch DOF between the short arm and the rotor and Y_R axis is perpendicular to both axes.
- Local coordinate system (X_P, Y_P, Z_P) of the parachute defined at the point of connection between the long arm and the parachute (point C, Figure 2). Z_P is parallel to the longitudinal axis of the parachute, X_P axis is parallel to the pitch DOF between the long arm and the parachute and Y_P axis is perpendicular to both axes.

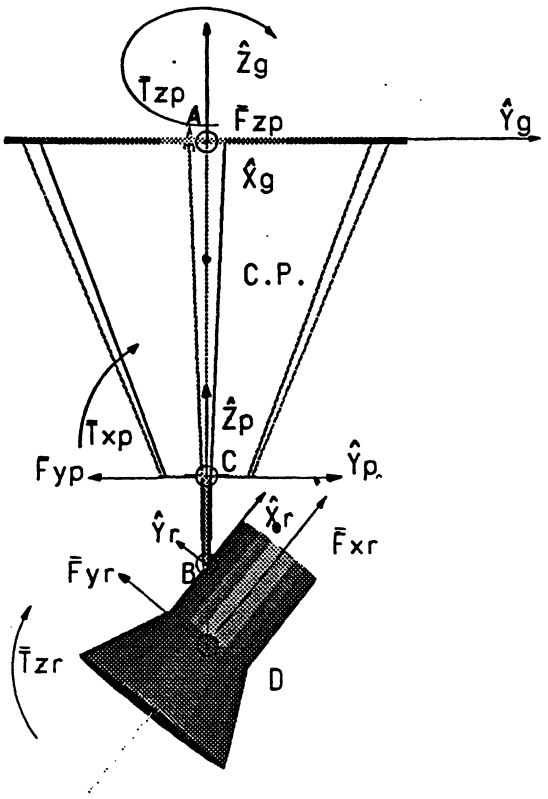

Figure 2 : Coordinate systems and external loads

AERODYNAMIC LOADS

The aerodynamic loads on the generalized parachute are calculated in respect to its lower point (point C, Figure 2) and are defined by the following equations:

$$
\begin{aligned}
& F_{ZP} = Q * S * C_{ZP} && \text{Drag force} \\
& F_{YP} = Q * S * C_{YP} * \beta_P && \text{Elevation force} \\
(1)\ & F_{XP} = Q * S * C_{XP} * \delta_P && \text{Elevation force} \\
& T_{XP} = Q*S*D*\{C_M*\beta_P+C_{MQ}*[D*(d\beta_P/dt)/2/V_P]+C_0\} && \text{Pitch torque} \\
& T_{YP} = Q*S*D*\{C_M*\delta_P+C_{MQ}*[D*(d\delta_P/dt)/2/V_P]\} && \text{Pitch torque} \\
& T_{ZP} = Q*S*D*[C_L+C_{LQ}*(D*n/2/V_P)] && \text{Rolling torque}
\end{aligned}
$$

where $Q=0.5*\rho*V_P^2$, ρ - air density, V_P - resultant velocity measured at center of pressure, S - equivalent cross area, D - equivalent diameter, n - rolling speed.
C_{XP}, C_{YP}, C_{ZP}, C_M, C_{MQ}, C_0, C_L and C_{LQ} are the aerodynamic coefficients measured in a wind tunnel (index $_Q$ refers to damping coefficients).
The angle of attack is defined by the following relations between the components of the parachute velocity V_P, measured at the pressure center and defined in parachute reference axes (X_P, Y_P, Z_P):

$$
\begin{aligned}
& \beta_P = \text{ARCTAN}\,(V_{YP} / V_{ZP}) && \text{angle of attack in } (Y_P, Z_P) \text{ plane} \\
(2)\ & \\
& \delta_P = \text{ARCSIN}\,(V_{XP} / V_P) && \text{angle of attack in (resultant } V_P \text{ direction, } X_P) \text{ plane}
\end{aligned}
$$

where d(angle)/dt - time derivative of the angle of attack.

The aerodynamic loads on the rotor are calculated in respect to its center of mass (point D, Figure 2) and are defined by the following expressions:

$$F_{XR} = Q * S * C_{XR} \qquad \text{Drag force}$$
$$(3)\ F_{YR} = Q * S * C_{YR} \qquad \text{Elevation force}$$
$$T_{ZR} = Q*S*D*\{C_{ZR} + C_{RQ}*[D*(d\beta_R/dt)/2/V_R]\} \qquad \text{Pitch torque}$$

where $Q=0.5*\rho* V_R^2$, V_R - velocity measured at center of mass. C_{XR}, C_{YR}, C_{ZR}, C_{RQ} are the aerodynamic coefficients measured in a wind tunnel. The angle of attack β_R is defined by the following relation between the components of V_R, measured at its center of mass and defined in the rotor reference axes (X_R, Y_R, Z_R). The other component of the angle of attack is neglected.

$$(4)\ \beta_R = \text{ARCTAN}\ (V_{YR} / V_{XR}) \qquad \text{angle of attack in } (Y_R, X_R) \text{ plane}$$

SCENARIOS for ANALYSIS

The analysis included evaluation of several cases of system stability sensitivity. It was observed from preliminary measurements that the system is sensitive to variations in moments of inertia. The principal moments of inertia are close to spherical configuration as a result of design constraints. The purpose of the analysis is to define the conditions for stable motion, where the stability is defined as small pitch oscillations of the rotor. The following cases have been tested and are described further on:

- Nominal case without the gap DOF and with balanced rotor.
- Effect of principal moment of inertia ratios on motion stability.
- Effect of dynamic unbalance , up to 50 [kg-mm^2], on motion stability.
- Effect of the extra gap DOF , of about 0.5[degs], on motion stability.

RESULTS

The major results of the various simulations are shown in Table 1 and Figures 3 and 4. Figure 3 shows the pitch angle, which is a measure of stability, for a stable and unstable cases. The unstable oscillations in Figure 3 represent a moments of inertia ratio of B/C = 0.87. A, B, C are principal moments of inertia around X_3, Y_3 and Z_3 axes respectively, Figure 5. The critical value for stable oscillations is B/C = 0.89. Smaller values of this ratio cause divergence of the oscillations. Figure 4 describes the trace of motion on ground for a stable case.

Adding imbalance of up to 50 [kg-mm^2], does not change the stability criteria.

The additional DOF that represent mechanical tolerances of about 0.5 [degs], improve the stable range of moments of inertia ratio to B/C = 0.7 and even less.

Table No. 1 : Comparison Between Various Results

Case	A / C	B / C	Descent velocity deviation from nominal [m/s]	Rolling Speed deviation from nominal [Hz]	Rotor pitch angle deviation from nominal β_R [degs]	Rotor Stable + / -	Parachute β_P [degs]	Parachute δ_P [degs]
Experiment	0.99	1.03	0	0.1	-1.6±2	+		
Nominal (1	0.99	1.03	0	0	0±0.07	+	1.7	0.45
Nominal (2	0.99	1.18	0	0	0.1±0.09	+	1.7	0.45
Nominal (3	0.89	1.03	0	-0.2	3.4±1.5	-	0.6±0.8	0.3
Include Unbalance (1	0.99	1.03	0.1	0.1	-1.0±0.1	+	-0.74	-2.0
Include Unbalance (2	0.99	1.18	0.1	0.1	-1.0±0.1	+	-0.74	-2.0
Include Unbalance (3	0.89	1.03	-0.2	-0.1	2.9±1.6	-	-0.7	0.2
Include Gap (1	0.99	1.03	-0.1	0	0.8±0.1	+	-1.6	-0.1
Include Gap (2	0.99	1.2	-0.1	0	0.8±0.1	+	-1.6	-0.1
Include Gap (3	0.7	1.03	-0.1	-0.1	3.6±0.1	+	-0.4	0.6
Include Gap & Unbalance (1	0.99	1.03	-0.1	0	-0.5±0.05	+	-2.0	-0.4
Include Gap & Unbalance (2	0.99	1.20	-0.1	0	-0.5±0.05	+	-2.0	-0.4
Include Gap & Unbalance (3	0.7	1.03	-0.1	-0.2	3.7±0.05	+	-0.4	0.25
Large Gap (1	0.99	1.03	-0.1	0	3.8±1.0	+	1.1	-0.8
(similar to (2	0.99	0.9	-0.1	0	3.4 ⇒ 9.4	-	2.8	0.5
Analytic Model)(3	0.8	1.03	-0.1	0	4.0±1.1	+	0.9	-0.6
Analytic model of a reduced system.	0.99	0.9	0	0		-		

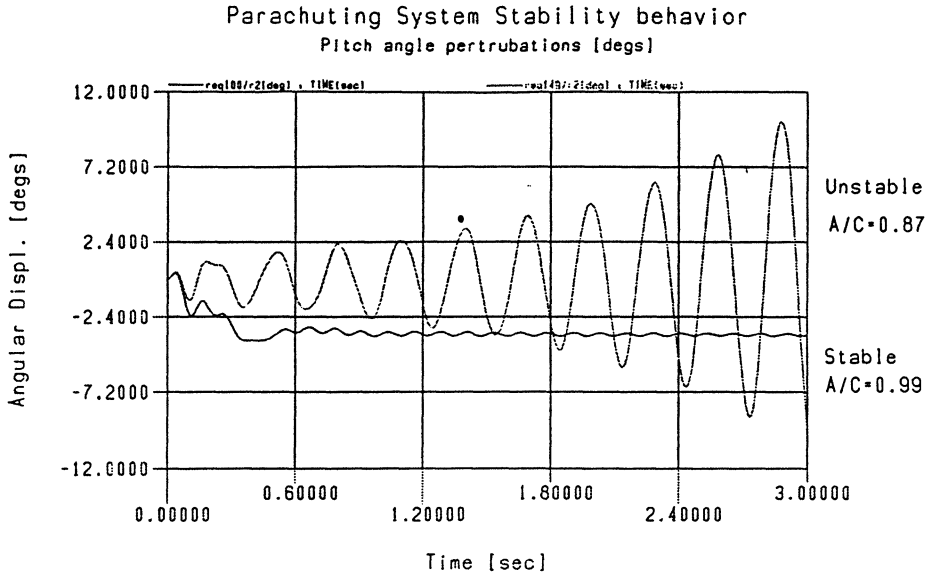

Figure 3 : Pitch angle oscillations as a function of moment of inertia ratios

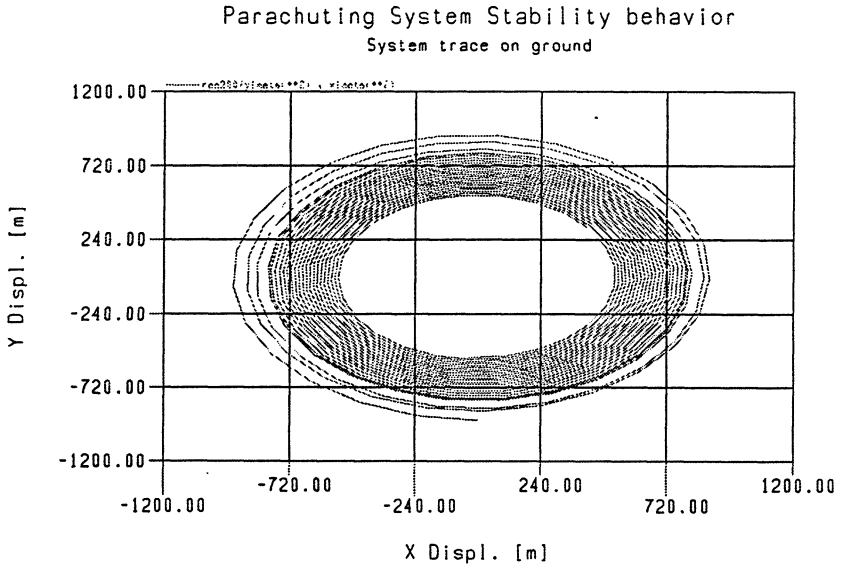

Figure 4 : Trace of a stable motion

COMPARISON to an ANALYTIC MODEL

Due to the large difference between the rotor and parachute masses, it is assumed that the rotor is the dominant part that affects and controls the stability of the system. Therefore an analytic model of the spinning rotor at constant speed n, hung on a universal joint (two DOF) was established, in order to compare its behavior to the complete model. A scheme of the model and coordinate systems are shown in Figure 5.

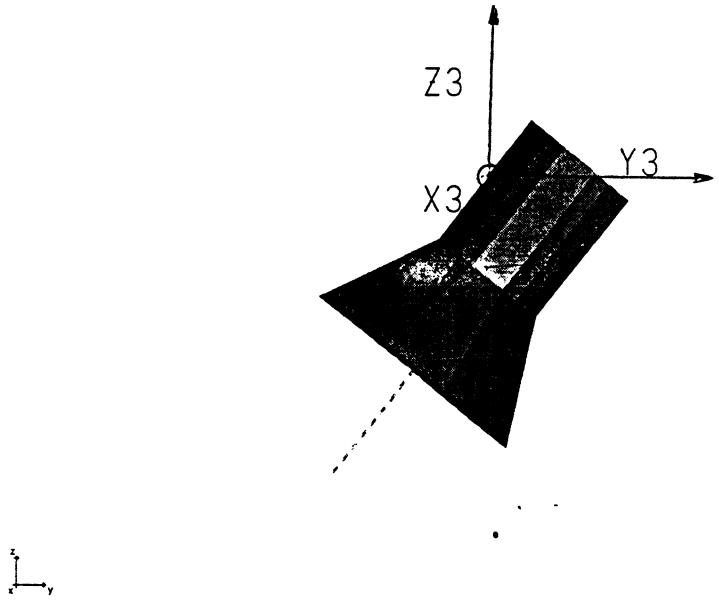

Figure 5 : Analytic Model and coordinate system

X, Y, Z - Inertial coordinate system,
X_3, Y_3, Z_3 - Coordinate system attached to the rotor,
n - constant angular velocity around Z axis, [rad / sec].
ψ - angle between the two arms of the universal joint around the rotated Y axis,
φ - Angle between the Rotor and the universal joint around X_3 axis.

A set of two equations of motion represent the relationships between angular displacements around the DOF, mass properties of the rotor and the external torques acting on its center of mass.

$$(5)\quad \begin{bmatrix} D^2A-(B-C)*n^2+m*g*L & -n*D*(A+B-C) \\ n*D*(A+B-C) & D^2B-(A-C)*n^2+m*g*L \end{bmatrix} \begin{pmatrix} \varphi \\ \psi \end{pmatrix} = \begin{pmatrix} -T_1 \\ T_2 \end{pmatrix}$$

where D denotes for d/dt; A, B, C are principal moments of inertia around X_3, Y_3 and Z_3 axes respectively; m - Rotor mass; L - distance of center of mass from the universal joint; g - acceleration of gravity; ψ, φ - the DOF; T_1, T_2 - external torques acting around axes X_3, Y_3 respectively.
The specific solutions for φ and ψ are

$$\varphi = T_1/[(B-C)*n^2-m*g*L]$$

(6)

$$\psi = -T_2/[(A-C)*n^2-m*g*L]$$

Certain relations between A, B, C, n, m and L may cause instability. Solving the homogeneous equations yield a 4th order polynomial equation

(7) $a_1 * p^4 + a_2 * p^2 + a_3 = 0$

where $a_1 = A * B$

$a_2 = (-C^2-2*A*B+A*C+B*C)*n^2 - m*g*L*(A+B)$

$a_3 = [(B-C)*n^2 - m*g*L] * [(A-C)*n^2 - m*g*L]$

p - natural frequencies

The stability range of Eq. (7) under the design constraint of A>C>B is

(8) $1.096 > (A / C) > 1$

$(B / C) < 1$

The stability criteria depends on the ratio between the large to middle moments of inertia. These results are different to those of the complete model where the stability is sensitive to the ratio between the small to middle moments of inertia.

CONCLUSIONS

The main conclusions of the analysis presented in this study are as follows:

- The stability of a parachuting system depends on the ratios of moments of inertia.
- Dynamic unbalance of the rotor in the specified range does not affect the stability of motion.
- Adding purposely more angular degrees of freedom by taking into account the gaps and manufacturing tolerances, increases the stability range by a significant amount, from B/C = 0.89 to 0.7 and even less.
- The analytic model is not accurate enough, although it includes most of the system's mass, since it does not include the complete number of DOF, non-linear effects as gap and impact phenomena and solution of large displacements. Instead, it consists of two angular DOF with a solution that defines a different criteria of instability. Changing the complete model so that the angular DOF are replaced by a universal DOF, results in a similar stability criteria as derived by the analytic model.
- The results achieved by the complete numerical model are in good agreement with the experimental results.